

C^1 Quadratic Interpolation of Meshes

David Eberly, Geometric Tools, Redmond WA 98052

<https://www.geometrictools.com/>

This work is licensed under the Creative Commons Attribution 4.0 International License. To view a copy of this license, visit <http://creativecommons.org/licenses/by/4.0/> or send a letter to Creative Commons, PO Box 1866, Mountain View, CA 94042, USA.

Created: March 2, 1999

Last Modified: April 7, 2018

Contents

1	Introduction	2
2	Mathematical Preliminaries	2
2.1	Barycentric Coordinates	2
2.2	Inscribed Centers	3
2.3	Bézier Triangles	5
2.4	Derivatives	6
2.5	Derivative Continuity	7
3	Globally C^1 Quadratic Height Field of Form $h = f(x_0, x_1)$ without Local Control	10
4	Globally C^1 Quadratic Height Field of Form $h = f(x_0, x_1)$ with Local Control	15
5	The Algorithm for Graphs of $f(x, y, z)$	19
6	The Algorithm for Surfaces	22

1 Introduction

This document describes the Cendes-Wong algorithm [2] for interpolating arbitrary point sets with elements $((x_i, y_i), f(x_i, y_i), f_x(x_i, y_i), f_y(x_i, y_i))$ for $0 \leq i < N$. The interpolating function $f(x, y)$ has continuous first-order derivatives. The points (x_i, y_i) are arbitrarily spaced. At each point (x_i, y_i) the user specifies the function value $f(x_i, y_i)$ and its two first-order partial derivatives $f_x(x_i, y_i)$ and $f_y(x_i, y_i)$. The outline of the algorithm is as follows.

1. *Triangulation.* The spatial points must be triangulated. Generally, one chooses a Delaunay triangulation; see [4].
2. *Subdivision.* Each triangle is subdivided into six triangles. The subdivision requires knowledge of the inscribed centers of the triangle and its three adjacent triangles.
3. *Bézier net construction.* Each subtriangle is further subdivided into four triangles. This subdivision is affine and the partition is used to build a quadratic function via the Bézier triangle method described in [3]. The quadratic function for a single triangle is, of course, a C^1 function, but additionally the interpolation is C^1 at the vertices and edges shared with other triangles.

The interpolator accepts as input a spatial location (x, y) and returns as output the interpolated values for $f(x, y)$, $f_x(x, y)$ and $f_y(x, y)$.

The reduced computation of this algorithm compared to that for cubic interpolators is attractive. The setup costs for the interpolation are assumed to be negligible compared to the cost of interpolation for a large number of input points. Because the interpolation guarantees only C^1 continuity, an application that requires C^2 continuity must use a different interpolation algorithm. This is true, for example, when the application requires smoothly varying normal vectors or must compute surface curvatures.

The interpolation has local control. If the function or derivative values are modified at a single data point, then the affine subdivision of the triangles sharing the data point does not change, but the function values at the control points generated by subdivision must be recomputed. If the spatial component of a single data point is modified, then the affine subdivisions of the triangles sharing the data point change. These changes are propagated to any immediately adjacent triangles of those which share the data point, but no farther.

I provide a generalization of the Cendes-Wong algorithm to graphs of functions $f(x, y, z, w)$. The ideas work in general dimensions. I also mention how you can apply the ideas to a 2-dimensional manifold triangle mesh as long as you have a package to generate 2-dimensional surface parameters (automatically generated texture coordinates, so to speak).

2 Mathematical Preliminaries

2.1 Barycentric Coordinates

Let a triangle have vertices \mathbf{p}_0 , \mathbf{p}_1 and \mathbf{p}_2 . Any point \mathbf{p} can be written as a linear combination of the triangle vertices,

$$\mathbf{p} = u_0\mathbf{p}_0 + u_1\mathbf{p}_1 + u_2\mathbf{p}_2, \quad u_0 + u_1 + u_2 = 1 \tag{1}$$

The coefficients (u_0, u_1, u_2) are the *barycentric coordinates of the point \mathbf{p} with respect to the triangle*. If \mathbf{p} is inside the triangle or on a triangle edge, we additionally know that $u_i \in [0, 1]$. If \mathbf{p} is outside the triangle, at least one of u_i is negative. The definition is independent of dimension; the vectors can be in \mathbb{R}^n for any $n \geq 2$.

Constructing u_0 , u_1 and u_2 is a matter of solving a system of linear equations. Subtracting \mathbf{p}_2 from the equation for \mathbf{p} , using $u_2 = 1 - u_0 - u_1$ and grouping terms leads to

$$\mathbf{p} - \mathbf{p}_2 = u_0(\mathbf{p}_0 - \mathbf{p}_2) + u_1(\mathbf{p}_1 - \mathbf{p}_2) \quad (2)$$

The vectors $\mathbf{p}_0 - \mathbf{p}_2$ and $\mathbf{p}_1 - \mathbf{p}_2$ are linearly independent because they are two edges of the same triangle. The linear independence also guarantees the linear system has a unique solution for u_0 and u_1 . Dot these vectors with equation (2) to obtain the linear system of equations

$$\begin{bmatrix} (\mathbf{p}_0 - \mathbf{p}_2) \cdot (\mathbf{p}_0 - \mathbf{p}_2) & (\mathbf{p}_0 - \mathbf{p}_2) \cdot (\mathbf{p}_1 - \mathbf{p}_2) \\ (\mathbf{p}_1 - \mathbf{p}_2) \cdot (\mathbf{p}_0 - \mathbf{p}_2) & (\mathbf{p}_1 - \mathbf{p}_2) \cdot (\mathbf{p}_1 - \mathbf{p}_2) \end{bmatrix} \begin{bmatrix} u_0 \\ u_1 \end{bmatrix} = \begin{bmatrix} (\mathbf{p}_0 - \mathbf{p}_2) \cdot (\mathbf{p} - \mathbf{p}_2) \\ (\mathbf{p}_1 - \mathbf{p}_2) \cdot (\mathbf{p} - \mathbf{p}_2) \end{bmatrix} \quad (3)$$

Although it is simple to solve the equation algebraically, the solution can be written geometrically as

$$u_0 = \frac{\text{Area}(\mathbf{p}, \mathbf{p}_1, \mathbf{p}_2)}{\text{Area}(\mathbf{p}_0, \mathbf{p}_1, \mathbf{p}_2)}, \quad u_1 = \frac{\text{Area}(\mathbf{p}_0, \mathbf{p}, \mathbf{p}_2)}{\text{Area}(\mathbf{p}_0, \mathbf{p}_1, \mathbf{p}_2)}, \quad u_2 = \frac{\text{Area}(\mathbf{p}_0, \mathbf{p}_1, \mathbf{p})}{\text{Area}(\mathbf{p}_0, \mathbf{p}_1, \mathbf{p}_2)} \quad (4)$$

where $\text{Area}(\cdot, \cdot, \cdot)$ is the area of the triangle formed by the input points.

Given two points \mathbf{q}_0 and \mathbf{q}_1 , the difference is a vector $\Delta = \mathbf{q}_1 - \mathbf{q}_0$. With respect to the aforementioned triangle with vertices \mathbf{p}_i , let (u_0, u_1, u_2) be the barycentric coordinates of \mathbf{q}_0 and let (v_0, v_1, v_2) be the barycentric coordinates of \mathbf{q}_1 . Define $d_i = u_i - v_i$; then

$$\begin{aligned} \Delta &= \mathbf{q}_1 - \mathbf{q}_0 \\ &= (u_0\mathbf{p}_0 + u_1\mathbf{p}_1 + u_2\mathbf{p}_2) - (v_0\mathbf{p}_0 + v_1\mathbf{p}_1 + v_2\mathbf{p}_2) \\ &= (u_0 - v_0)\mathbf{p}_0 + (u_1 - v_1)\mathbf{p}_1 + (u_2 - v_2)\mathbf{p}_2 \\ &= d_0\mathbf{p}_0 + d_1\mathbf{p}_1 + d_2\mathbf{p}_2, \quad d_0 + d_1 + d_2 = 0 \end{aligned} \quad (5)$$

The coefficients (d_0, d_1, d_2) are referred to as the *barycentric coordinates of the vector Δ with respect to the triangle*. The sum of barycentric coordinates for a point is 1 and the sum of barycentric coordinates for a vector is 0.

2.2 Inscribed Centers

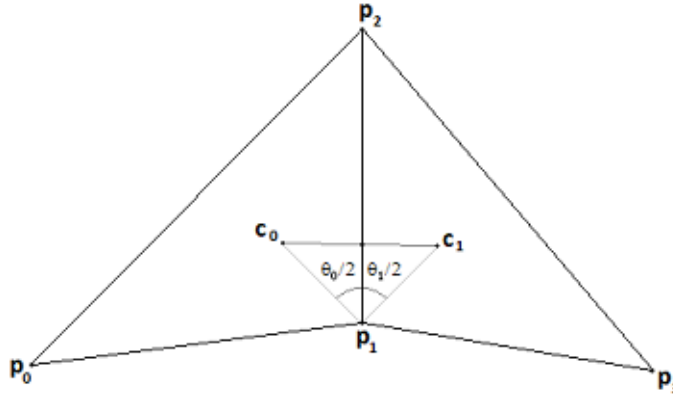
Let a triangle have vertices \mathbf{p}_0 , \mathbf{p}_1 and \mathbf{p}_2 . The inscribed circle has radius r and center $\mathbf{c} = u_0\mathbf{p}_0 + u_1\mathbf{p}_1 + u_2\mathbf{p}_2$ for barycentric coordinates (u_0, u_1, u_2) . The subtriangle $\langle \mathbf{c}, \mathbf{p}_1, \mathbf{p}_2 \rangle$ has base length $|\mathbf{p}_1 - \mathbf{p}_2|$ and height r , so its area is $\text{Area}(\mathbf{c}, \mathbf{p}_1, \mathbf{p}_2) = |\mathbf{p}_1 - \mathbf{p}_2|r/2$. Similarly, the two other subtriangles have areas $\text{Area}(\mathbf{p}_0, \mathbf{c}, \mathbf{p}_2) = |\mathbf{p}_0 - \mathbf{p}_2|r/2$ and $\text{Area}(\mathbf{p}_0, \mathbf{p}_1, \mathbf{c}) = |\mathbf{p}_0 - \mathbf{p}_1|r/2$. The triangle area is the sum of the areas of the three subtriangles, $\text{Area}(\mathbf{p}_0, \mathbf{p}_1, \mathbf{p}_2) = (|\mathbf{p}_1 - \mathbf{p}_2| + |\mathbf{p}_0 - \mathbf{p}_2| + |\mathbf{p}_0 - \mathbf{p}_1|)r/2$. Using equation (4), The barycentric coordinates of the center of the inscribed circle are

$$\begin{aligned} u_0 &= |\mathbf{p}_1 - \mathbf{p}_2| / (|\mathbf{p}_1 - \mathbf{p}_2| + |\mathbf{p}_0 - \mathbf{p}_2| + |\mathbf{p}_0 - \mathbf{p}_1|) \\ u_1 &= |\mathbf{p}_0 - \mathbf{p}_2| / (|\mathbf{p}_1 - \mathbf{p}_2| + |\mathbf{p}_0 - \mathbf{p}_2| + |\mathbf{p}_0 - \mathbf{p}_1|) \\ u_2 &= |\mathbf{p}_0 - \mathbf{p}_1| / (|\mathbf{p}_1 - \mathbf{p}_2| + |\mathbf{p}_0 - \mathbf{p}_2| + |\mathbf{p}_0 - \mathbf{p}_1|) \end{aligned} \quad (6)$$

which are ratios of the lengths of the triangle edges to the triangle perimeter.

A ray from a triangle vertex \mathbf{p}_i to the center \mathbf{c} bisects the angle formed by the two edges sharing \mathbf{p}_i . A consequence is that the segment connecting the centers of two adjacent triangles must intersect the common edge of the triangles at an interior point of the edge, a fact used in the subdivision algorithm. The proof is as follows. If two adjacent triangles form a convex quadrilateral, the segment connecting the centers clearly intersects the shared edge at an interior point. The intersection property is not as clear when the triangles form a nonconvex quadrilateral such as the one shown in figure 1.

Figure 1. For adjacent triangles that do not form a convex quadrilateral, is it always true that the segment connecting inscribed centers intersects the interior of the common edge?



The inscribed centers are \mathbf{c}_0 and \mathbf{c}_1 . Set up the intersection equations as

$$(1-t)\mathbf{p}_1 + t\mathbf{p}_2 = (1-s)\mathbf{c}_0 + s\mathbf{c}_1 \quad (7)$$

The centers lie on different sides of the line containing the common edge $\langle \mathbf{p}_1, \mathbf{p}_2 \rangle$, so the segment connecting the centers must intersect that line at an interior point of the segment, which implies $0 < s < 1$. The line containing the common edge has origin \mathbf{p}_1 and direction $\mathbf{p}_2 - \mathbf{p}_1$. The intersection of the segment $\langle \mathbf{c}_0, \mathbf{c}_1 \rangle$ with the line must occur below \mathbf{p}_2 , which implies $t < 1$. If we can additionally prove that $t > 0$, then the segment connecting the inscribed centers must intersect the interior of the common triangle edge.

In figure 1, the angle at \mathbf{p}_1 between the edge direction vectors $\mathbf{p}_0 - \mathbf{p}_1$ and $\mathbf{p}_2 - \mathbf{p}_1$ is θ_0 . $\mathbf{c}_0 - \mathbf{p}_1$ bisects the angle θ_0 at \mathbf{p}_1 . We know that $0 < \theta_0 < \pi$, so $0 < \theta_0/2 < \pi/2$ and $\cos(\theta_0/2) > 0$. Similarly, the angle at \mathbf{p}_1 between the edge direction vectors $\mathbf{p}_2 - \mathbf{p}_1$ and $\mathbf{p}_3 - \mathbf{p}_1$ is θ_1 and $\mathbf{c}_1 - \mathbf{p}_1$ bisects the angle θ_1 at \mathbf{p}_1 . We know that $0 < \theta_1 < \pi$, so $0 < \theta_1/2 < \pi/2$ and $\cos(\theta_1/2) > 0$. In equation 7, subtract \mathbf{p}_1 and dot with $\mathbf{p}_2 - \mathbf{p}_1$ to obtain

$$\begin{aligned} t|\mathbf{p}_2 - \mathbf{p}_1|^2 &= (1-s)[(\mathbf{c}_0 - \mathbf{p}_1) \cdot (\mathbf{p}_2 - \mathbf{p}_1)] + s[(\mathbf{c}_1 - \mathbf{p}_1) \cdot (\mathbf{p}_2 - \mathbf{p}_1)] \\ &= (1-s)[|\mathbf{c}_0 - \mathbf{p}_1||\mathbf{p}_2 - \mathbf{p}_1| \cos(\theta_0/2)] + s[|\mathbf{c}_1 - \mathbf{p}_1||\mathbf{p}_2 - \mathbf{p}_1| \cos(\theta_1/2)] \\ &> 0 \end{aligned} \quad (8)$$

The positivity of $t|\mathbf{p}_2 - \mathbf{p}_1|^2$ is guaranteed because we know that $0 < s < 1$, $\cos(\theta_0/2) > 0$ and $\cos(\theta_1/2) > 0$. Consequently, $t > 0$ is guaranteed.

2.3 Bézier Triangles

Define a *multiindex on three indices* as $I = (i_0, i_1, i_2)$ and define $|I| = i_0 + i_1 + i_2$. Consider a collection of multiindexed points, each written as $\mathbf{b}_I = \mathbf{b}_{(i_0, i_1, i_2)}$ where $|I| = n$ for some specified $n \geq 0$. In this document, $n \leq 2$, so for simplicity of notation the point is written as $\mathbf{b}_{i_0 i_1 i_2}$. The collection can be organized as a triangular array. When $n = 0$, we have a single point \mathbf{b}_{000} . When $n = 1$, we have the triangular array

$$\begin{array}{c} \mathbf{b}_{001} \\ \mathbf{b}_{100} \quad \mathbf{b}_{010} \end{array} \quad (9)$$

When $n = 2$, we have the triangular array

$$\begin{array}{c} \mathbf{b}_{002} \\ \mathbf{b}_{101} \quad \mathbf{b}_{011} \\ \mathbf{b}_{200} \quad \mathbf{b}_{110} \quad \mathbf{b}_{020} \end{array} \quad (10)$$

The organization is chosen so that the bottom row corresponds to $i_2 = 0$, the row above it $i_1 = 1$, and so on. Within each row, the i_0 index decreases by 1 and the i_1 index increases by 1 as you traverse the elements of the row.

Define the multiindices $E_0 = (1, 0, 0)$, $E_1 = (0, 1, 0)$ and $E_2 = (0, 0, 1)$. Given a triangular array of points $\mathbf{b}_I \in \mathbb{R}^3$ where $|I| = n$, and given a barycentric coordinate $\mathbf{u} = (u_0, u_1, u_2)$, recursively define

$$\mathbf{b}_I^0(\mathbf{u}) = \mathbf{b}_I \quad (11)$$

and

$$\mathbf{b}_J^r(\mathbf{u}) = \sum_{k=0}^2 u_k \mathbf{b}_{J+E_k}^{r-1}(\mathbf{u}) \quad (12)$$

where $1 \leq r \leq n$ and J is a multiindex with $|J| = n - r$. When $r = n$, the point $\mathbf{b}_{(0,0,0)}^n(\mathbf{u})$ may be written more concisely by omitting the multiindex, $\mathbf{b}^n(\mathbf{u})$, and this point is on a surface called a *Bézier triangle patch* determined by the original array. The iterative algorithm of equations (11) and (12) is called the *de Casteljau algorithm*.

When $n = 1$ we must have $r = 1$. The de Casteljau algorithm produces

$$\mathbf{b}^1(\mathbf{u}) = \mathbf{b}_{000}^1(\mathbf{u}) = u_0 \mathbf{b}_{100} + u_1 \mathbf{b}_{010} + u_2 \mathbf{b}_{001} = \begin{bmatrix} \mathbf{b}_{100} & \mathbf{b}_{010} & \mathbf{b}_{001} \end{bmatrix} \begin{bmatrix} u_0 \\ u_1 \\ u_2 \end{bmatrix} \quad (13)$$

When $n = 2$, the case relevant to the Cendes-Wong algorithm, the triangle array is organized according to equation (9). For $r = 1$, the de Casteljau algorithm produces

$$\begin{aligned} \mathbf{b}_{100}^1(\mathbf{u}) &= u_0 \mathbf{b}_{200} + u_1 \mathbf{b}_{110} + u_2 \mathbf{b}_{101} \\ \mathbf{b}_{010}^1(\mathbf{u}) &= u_0 \mathbf{b}_{110} + u_1 \mathbf{b}_{020} + u_2 \mathbf{b}_{011} \\ \mathbf{b}_{001}^1(\mathbf{u}) &= u_0 \mathbf{b}_{101} + u_1 \mathbf{b}_{011} + u_2 \mathbf{b}_{002} \end{aligned} \quad (14)$$

For $r = 2$, the de Casteljau algorithm produces

$$\mathbf{b}^2(\mathbf{u}) = \mathbf{b}_{000}^2(\mathbf{u}) = u_0 \mathbf{b}_{100}^1(\mathbf{u}) + u_1 \mathbf{b}_{010}^1(\mathbf{u}) + u_2 \mathbf{b}_{001}^1(\mathbf{u}) = \begin{bmatrix} u_0 & u_1 & u_2 \end{bmatrix} \begin{bmatrix} \mathbf{b}_{200} & \mathbf{b}_{110} & \mathbf{b}_{101} \\ \mathbf{b}_{110} & \mathbf{b}_{020} & \mathbf{b}_{011} \\ \mathbf{b}_{101} & \mathbf{b}_{011} & \mathbf{b}_{002} \end{bmatrix} \begin{bmatrix} u_0 \\ u_1 \\ u_2 \end{bmatrix} \quad (15)$$

which is a quadratic function in the barycentric coordinates.

2.4 Derivatives

Let $\mathbf{b}(\mathbf{u})$ define points on a surface parameterized by barycentric coordinates $\mathbf{u} = (u_0, u_1, u_2)$ with $u_0 + u_1 + u_2 = 1$. The Bézier triangle is one such surface. The surface is 2-dimensional, so a typical parameterization involves 2 variables, say $\tilde{\mathbf{b}}(u_0, u_1) = \mathbf{b}(u_0, u_1, u_2) = \mathbf{b}(u_0, u_1, 1 - u_0 - u_2)$. The first-order partial derivatives of $\tilde{\mathbf{b}}$ are tangent vectors to the surface. Using the chain rule,

$$\tilde{\mathbf{b}}_{u_0} = \frac{\partial \tilde{\mathbf{b}}}{\partial u_0} = \frac{\partial \mathbf{b}}{\partial u_0} - \frac{\partial \mathbf{b}}{\partial u_2} = \mathbf{b}_{u_0} - \mathbf{b}_{u_2}, \quad \tilde{\mathbf{b}}_{u_1} = \frac{\partial \tilde{\mathbf{b}}}{\partial u_1} = \frac{\partial \mathbf{b}}{\partial u_1} - \frac{\partial \mathbf{b}}{\partial u_2} = \mathbf{b}_{u_1} - \mathbf{b}_{u_2} \quad (16)$$

where the notation \mathbf{y}_v denotes the first-order partial derivative $\partial \mathbf{y} / \partial v$. Using the chain rule again, the second-order partial derivatives of the surface are

$$\tilde{\mathbf{b}}_{u_0 u_0} = \mathbf{b}_{u_0 u_0} - 2\mathbf{b}_{u_0 u_2} + \mathbf{b}_{u_2 u_2}, \quad \tilde{\mathbf{b}}_{u_0 u_1} = \mathbf{b}_{u_0 u_1} - \mathbf{b}_{u_0 u_2} - \mathbf{b}_{u_1 u_2} + \mathbf{b}_{u_2 u_2}, \quad \tilde{\mathbf{b}}_{u_1 u_1} = \mathbf{b}_{u_1 u_1} - 2\mathbf{b}_{u_1 u_2} + \mathbf{b}_{u_2 u_2} \quad (17)$$

where the notation $\mathbf{y}_{v_0 v_1}$ denotes the second-order partial derivative $\partial^2 \mathbf{y} / \partial v_0 \partial v_1$.

Assuming the common case that the first-order partial derivatives are linearly independent tangent vectors, the tangent plane at a point is the span of these derivatives. A tangent vector is a linear combination

$$\begin{bmatrix} \tilde{\mathbf{b}}_{u_0} & \tilde{\mathbf{b}}_{u_1} \end{bmatrix} \begin{bmatrix} d_0 \\ d_1 \end{bmatrix} = \begin{bmatrix} \mathbf{b}_{u_0}(\mathbf{u}) & \mathbf{b}_{u_1}(\mathbf{u}) & \mathbf{b}_{u_2}(\mathbf{u}) \end{bmatrix} \begin{bmatrix} d_0 \\ d_1 \\ d_2 \end{bmatrix} = D_{\mathbf{d}}^1 \mathbf{b}(\mathbf{u}) \quad (18)$$

where $d_2 = -(d_0 + d_1)$ in which case $d_0 + d_1 + d_2 = 0$; that is, a tangent vector is a barycentric combination of the first-order partial derivatives of \mathbf{x} . The last equality defines the first-order differential operator $D_{\mathbf{d}}^1$ that applies to surfaces parameterized by barycentric coordinates. The direction is specified by its barycentric coordinates $\mathbf{d} = (d_0, d_1, d_2)$.

The second-order directional derivative in a specified direction for the parameterized surface is

$$\begin{bmatrix} d_0 & d_1 \end{bmatrix} \begin{bmatrix} \tilde{\mathbf{b}}_{u_0 u_0} & \tilde{\mathbf{b}}_{u_0 u_1} \\ \tilde{\mathbf{b}}_{u_0 u_1} & \tilde{\mathbf{b}}_{u_1 u_1} \end{bmatrix} \begin{bmatrix} d_0 \\ d_1 \end{bmatrix} = \begin{bmatrix} d_0 & d_1 & d_2 \end{bmatrix} \begin{bmatrix} \mathbf{b}_{u_0 u_0}(\mathbf{u}) & \mathbf{b}_{u_0 u_1}(\mathbf{u}) & \mathbf{b}_{u_0 u_2}(\mathbf{u}) \\ \mathbf{b}_{u_1 u_0}(\mathbf{u}) & \mathbf{b}_{u_1 u_1}(\mathbf{u}) & \mathbf{b}_{u_1 u_2}(\mathbf{u}) \\ \mathbf{b}_{u_2 u_0}(\mathbf{u}) & \mathbf{b}_{u_2 u_1}(\mathbf{u}) & \mathbf{b}_{u_2 u_2}(\mathbf{u}) \end{bmatrix} \begin{bmatrix} d_0 \\ d_1 \\ d_2 \end{bmatrix} = D_{\mathbf{d}}^2 \mathbf{b}(\mathbf{u}) \quad (19)$$

The last equality defines the second-order differential operator $D_{\mathbf{d}}^2$ that applies to surfaces parameterized by barycentric coordinates. The direction is specified by its barycentric coordinates $\mathbf{d} = (d_0, d_1, d_2)$.

A general formulation for directional derivatives of any order uses Bernstein polynomials and multiindices $I = (i_0, i_1, i_2)$,

$$B_I^n(\mathbf{d}) = \frac{n!}{i_0! i_1! i_2!} d_0^{i_0} d_1^{i_1} d_2^{i_2} \quad (20)$$

where $n = |I| = i_0 + i_1 + i_2$. The r^{th} -order directional derivative is

$$D_{\mathbf{d}}^r \mathbf{b}(\mathbf{u}) = \sum_{|I|=r} \partial^I \mathbf{b}(\mathbf{u}) B_I^r(\mathbf{d}) \quad (21)$$

where $I = (i_0, i_1, i_2)$ and $\partial^I \mathbf{b}(\mathbf{u}) = \partial^{i_0} \mathbf{b}(\mathbf{u}) / \partial u_0^{i_0} \partial u_1^{i_1} \partial u_2^{i_2}$. For a Bézier triangle $\mathbf{b}(\mathbf{u}) = \mathbf{b}^n(\mathbf{u})$, the r^{th} -order directional derivative is given in terms of de Casteljau iterates and Bernstein polynomials by

$$D_{\mathbf{d}}^r \mathbf{b}^n(\mathbf{u}) = \frac{n!}{(n-r)!} \sum_{|I|=r} \mathbf{b}_I^{n-r}(\mathbf{u}) B_I^r(\mathbf{d}) \quad (22)$$

For the quadratic case $n = 2$, the first-order directional derivatives of $\mathbf{b}^2(\mathbf{u})$ in the direction \mathbf{d} are

$$D_{\mathbf{d}}^1 \mathbf{b}^2(\mathbf{u}) = 2 \begin{bmatrix} u_0 & u_1 & u_2 \end{bmatrix} \begin{bmatrix} \mathbf{b}_{200} & \mathbf{b}_{110} & \mathbf{b}_{101} \\ \mathbf{b}_{110} & \mathbf{b}_{020} & \mathbf{b}_{011} \\ \mathbf{b}_{101} & \mathbf{b}_{011} & \mathbf{b}_{002} \end{bmatrix} \begin{bmatrix} d_0 \\ d_1 \\ d_2 \end{bmatrix} \quad (23)$$

and the second-order directional derivatives of $\mathbf{b}^2(\mathbf{u})$ in the direction \mathbf{d} are

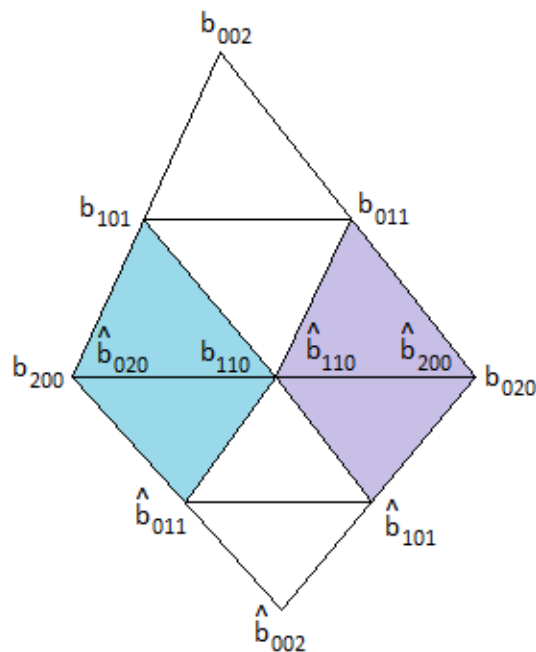
$$D_{\mathbf{d}}^2 \mathbf{b}^2(\mathbf{u}) = 2 \begin{bmatrix} d_0 & d_1 & d_2 \end{bmatrix} \begin{bmatrix} \mathbf{b}_{200} & \mathbf{b}_{110} & \mathbf{b}_{101} \\ \mathbf{b}_{110} & \mathbf{b}_{020} & \mathbf{b}_{011} \\ \mathbf{b}_{101} & \mathbf{b}_{011} & \mathbf{b}_{002} \end{bmatrix} \begin{bmatrix} d_0 \\ d_1 \\ d_2 \end{bmatrix} \quad (24)$$

The second derivative is constant with respect to u_0 , u_1 and u_2 as expected for a quadratic function.

2.5 Derivative Continuity

A comprehensive development of derivative continuity on the common boundary between two adjacent triangular patches is provided in [3]. The main result is that derivatives up through order r of $\mathbf{b}^n(\mathbf{u})$ depend only on the shared row of control points on the boundary and the r rows of control points adjacent to that boundary. I discuss only the cases relevant to the quadratic interpolation, namely, $r = 0$ and $r = 1$. Figure 2 illustrates two adjacent triangle patches. The top patch has control points \mathbf{b}_I and the bottom patch has control points $\hat{\mathbf{b}}_I$.

Figure 2. The domain triangles for adjacent Bézier triangle patches are shown here. The 3D control points shared by the two patches are \mathbf{b}_{200} , \mathbf{b}_{110} and \mathbf{b}_{020} . The first row of adjacent control points for the top patch are \mathbf{b}_{101} and \mathbf{b}_{011} . The first row of adjacent control points for the bottom patch are $\hat{\mathbf{b}}_{101}$ and $\hat{\mathbf{b}}_{011}$.



The figure shows a top-down view of the triangles $\langle \mathbf{b}_{200}, \mathbf{b}_{020}, \mathbf{b}_{002} \rangle$ and $\langle \hat{\mathbf{b}}_{200}, \hat{\mathbf{b}}_{020}, \hat{\mathbf{b}}_{002} \rangle$, but the two triangles are generally not coplanar.

Using equation (15), the patches define two quadratic functions, one for each domain triangle,

$$\mathbf{b}^2(\mathbf{u}) = \begin{bmatrix} u_0 & u_1 & u_2 \end{bmatrix} \begin{bmatrix} \mathbf{b}_{200} & \mathbf{b}_{110} & \mathbf{b}_{101} \\ \mathbf{b}_{110} & \mathbf{b}_{020} & \mathbf{b}_{011} \\ \mathbf{b}_{101} & \mathbf{b}_{011} & \mathbf{b}_{002} \end{bmatrix} \begin{bmatrix} u_0 \\ u_1 \\ u_2 \end{bmatrix} \quad (25)$$

where $u_0 + u_1 + u_2 = 1$ and

$$\hat{\mathbf{b}}^2(\hat{\mathbf{u}}) = \begin{bmatrix} \hat{u}_0 & \hat{u}_1 & \hat{u}_2 \end{bmatrix} \begin{bmatrix} \hat{\mathbf{b}}_{200} & \hat{\mathbf{b}}_{110} & \hat{\mathbf{b}}_{101} \\ \hat{\mathbf{b}}_{110} & \hat{\mathbf{b}}_{020} & \hat{\mathbf{b}}_{011} \\ \hat{\mathbf{b}}_{101} & \hat{\mathbf{b}}_{011} & \hat{\mathbf{b}}_{002} \end{bmatrix} \begin{bmatrix} \hat{u}_0 \\ \hat{u}_1 \\ \hat{u}_2 \end{bmatrix} \quad (26)$$

where $\hat{u}_0 + \hat{u}_1 + \hat{u}_2 = 1$. The graphs of the functions terminate in quadratic curves when $u_2 = 0$ and $\hat{u}_2 = 0$, which occurs at the shared edge of the domain triangles. The quadratic curves are guaranteed to be the same when the control points are the same,

$$\hat{\mathbf{b}}_{200} = \mathbf{b}_{020}, \quad \hat{\mathbf{b}}_{110} = \mathbf{b}_{110}, \quad \hat{\mathbf{b}}_{020} = \mathbf{b}_{200} \quad (27)$$

in which case the surface for the pair of patches is continuous along the shared edge.

Establishing conditions for the continuity of the derivatives along the shared edge requires more work. Effectively, we must reparameterize $\hat{\mathbf{b}}(\mathbf{u})$ in terms of \mathbf{u} in order to compute the derivatives of $\hat{\mathbf{b}}(\mathbf{u})$ in terms of \mathbf{u} rather than $\hat{\mathbf{u}}$. The approach uses the concept of *domain triangles* that live in 2D (the domain plane), whereas the triangle patch lives in 3D. Imagine a triangle in the domain plane, say, $\langle \mathbf{x}_{200}, \mathbf{x}_{020}, \mathbf{x}_{002} \rangle$ with barycentric coordinates that define points $\mathbf{x}(\mathbf{u}) = u_0 \mathbf{x}_{200} + u_1 \mathbf{x}_{020} + u_2 \mathbf{x}_{002}$. The domain triangle maps naturally to the 3D triangle $\langle \mathbf{b}_{200}, \mathbf{b}_{020}, \mathbf{b}_{002} \rangle$ by $\mathbf{b}^1(\mathbf{u}) = u_0 \mathbf{b}_{200} + u_1 \mathbf{b}_{020} + u_2 \mathbf{b}_{002}$. Similarly, $\langle \hat{\mathbf{x}}_{200}, \hat{\mathbf{x}}_{020}, \hat{\mathbf{x}}_{002} \rangle$ is a domain triangle with barycentric coordinates $\hat{\mathbf{u}}$ that maps to the 3D triangle $\langle \hat{\mathbf{b}}_{200}, \hat{\mathbf{b}}_{020}, \hat{\mathbf{b}}_{002} \rangle$; that is, $\hat{\mathbf{x}}(\hat{\mathbf{u}}) = \hat{u}_0 \hat{\mathbf{x}}_{200} + \hat{u}_1 \hat{\mathbf{x}}_{020} + \hat{u}_2 \hat{\mathbf{x}}_{002}$ maps to $\hat{\mathbf{b}}^1(\hat{\mathbf{u}}) = \hat{u}_0 \hat{\mathbf{b}}_{200} + \hat{u}_1 \hat{\mathbf{b}}_{020} + \hat{u}_2 \hat{\mathbf{b}}_{002}$.

Figure 2 shows the \mathbf{x} -triangle as the top patch and the $\hat{\mathbf{x}}$ -triangle as the bottom patch. Firstly, we can write $\hat{\mathbf{x}}_{002}$ as a barycentric combination of the vertices of the top domain triangle,

$$\hat{\mathbf{x}}_{002} = v_0 \mathbf{x}_{200} + v_1 \mathbf{x}_{020} + v_2 \mathbf{x}_{002} \quad (28)$$

for some (v_0, v_1, v_2) with $v_0 + v_1 + v_2 = 1$ and $v_2 \neq 0$. The last condition is a consequence of $\hat{\mathbf{x}}_{002}$ living strictly outside the top domain triangle. Secondly, a point $\hat{\mathbf{x}}$ in the bottom domain triangle can be written as

$$\begin{aligned} \hat{\mathbf{x}} &= \hat{u}_0 \hat{\mathbf{x}}_{200} + \hat{u}_1 \hat{\mathbf{x}}_{020} + \hat{u}_2 \hat{\mathbf{x}}_{002}, \text{ barycentric combination in bottom domain triangle} \\ &= \hat{u}_0 \mathbf{x}_{020} + \hat{u}_1 \mathbf{x}_{200} + \hat{u}_2 \hat{\mathbf{x}}_{002}, \text{ using equation (27)} \\ &= \hat{u}_0 \mathbf{x}_{020} + \hat{u}_1 \mathbf{x}_{200} + \hat{u}_2 (v_0 \mathbf{x}_{200} + v_1 \mathbf{x}_{020} + v_2 \mathbf{x}_{002}), \text{ using equation (28)} \\ &= (\hat{u}_1 + \hat{u}_2 v_0) \mathbf{x}_{200} + (\hat{u}_0 + \hat{u}_2 v_1) \mathbf{x}_{020} + (\hat{u}_2 v_2) \mathbf{x}_{002} \\ &= u_0 \mathbf{x}_{200} + u_1 \mathbf{x}_{020} + u_2 \mathbf{x}_{002}, \text{ barycentric combination in top domain triangle} \end{aligned} \quad (29)$$

Therefore,

$$(\hat{u}_0, \hat{u}_1, \hat{u}_2) = (u_1 - u_2 v_1 / v_2, u_0 - u_2 v_0 / v_2, u_2 / v_2) \quad (30)$$

Let $\Delta = d_0 \mathbf{x}_{200} + d_1 \mathbf{x}_{020} + d_2 \mathbf{x}_{002}$ be a direction vector for which we want to evaluate the derivative $D_{\mathbf{d}}^1 \mathbf{b}^2(\mathbf{u})$, where $\mathbf{d} = (d_0, d_1, d_2)$ are the barycentric coordinates of the direction with respect to the top domain triangle with $d_0 + d_1 + d_2 = 0$ and $d_2 \neq 0$. The direction can be written as a barycentric combination with respect to the bottom domain triangle, $\Delta = \hat{d}_0 \hat{\mathbf{x}}_{200} + \hat{d}_1 \hat{\mathbf{x}}_{020} + \hat{d}_2 \hat{\mathbf{x}}_{002}$ where $\hat{\mathbf{d}} = (\hat{d}_0, \hat{d}_1, \hat{d}_2)$ with $\hat{d}_0 + \hat{d}_1 + \hat{d}_2 = 0$ and $\hat{d}_2 \neq 0$. We can use this to evaluate the derivative $D_{\hat{\mathbf{d}}}^1 \hat{\mathbf{b}}^2(\hat{\mathbf{u}})$. Using the same argument as in equation (29), the barycentric coordinates for the direction vector are related by

$$(\hat{d}_0, \hat{d}_1, \hat{d}_2) = (d_1 - d_2 v_1 / v_2, d_0 - d_2 v_0 / v_2, d_2 / v_2) \quad (31)$$

The goal now is to determine conditions on the control points for which the derivative

$$D_{\mathbf{d}} \mathbf{b}^2(\mathbf{u}) = 2 \begin{bmatrix} u_0 & u_1 & u_2 \end{bmatrix} \begin{bmatrix} \mathbf{b}_{200} & \mathbf{b}_{110} & \mathbf{b}_{101} \\ \mathbf{b}_{110} & \mathbf{b}_{020} & \mathbf{b}_{011} \\ \mathbf{b}_{101} & \mathbf{b}_{011} & \mathbf{b}_{002} \end{bmatrix} \begin{bmatrix} d_0 \\ d_1 \\ d_2 \end{bmatrix} \quad (32)$$

and the derivative

$$D_{\hat{\mathbf{d}}} \hat{\mathbf{b}}^2(\hat{\mathbf{u}}) = 2 \begin{bmatrix} \hat{u}_0 & \hat{u}_1 & \hat{u}_2 \end{bmatrix} \begin{bmatrix} \hat{\mathbf{b}}_{200} & \hat{\mathbf{b}}_{110} & \hat{\mathbf{b}}_{101} \\ \hat{\mathbf{b}}_{110} & \hat{\mathbf{b}}_{020} & \hat{\mathbf{b}}_{011} \\ \hat{\mathbf{b}}_{101} & \hat{\mathbf{b}}_{011} & \hat{\mathbf{b}}_{002} \end{bmatrix} \begin{bmatrix} \hat{d}_0 \\ \hat{d}_1 \\ \hat{d}_2 \end{bmatrix} \quad (33)$$

are equal for every point on the shared edge $u_2 = 0 = \hat{u}_2$. Parameterize the shared edge by $u_0 = t$ and $u_1 = 1 - t$ for $t \in [0, 1]$. Using continuity along the shared edge, the parameterization for that edge, equation (30) and equation (31),

$$\begin{aligned} & \begin{bmatrix} t & 1-t & 0 \end{bmatrix} \begin{bmatrix} \mathbf{b}_{200} & \mathbf{b}_{110} & \mathbf{b}_{101} \\ \mathbf{b}_{110} & \mathbf{b}_{020} & \mathbf{b}_{011} \\ \mathbf{b}_{101} & \mathbf{b}_{011} & \mathbf{b}_{002} \end{bmatrix} \begin{bmatrix} d_0 \\ d_1 \\ d_2 \end{bmatrix} \\ &= \begin{bmatrix} 1-t & t & 0 \end{bmatrix} \begin{bmatrix} \mathbf{b}_{020} & \mathbf{b}_{110} & \hat{\mathbf{b}}_{101} \\ \mathbf{b}_{110} & \mathbf{b}_{200} & \hat{\mathbf{b}}_{011} \\ \hat{\mathbf{b}}_{101} & \hat{\mathbf{b}}_{011} & \hat{\mathbf{b}}_{002} \end{bmatrix} \begin{bmatrix} d_1 - v_1 d_2 / v_2 \\ d_0 - v_0 d_2 / v_2 \\ d_2 / v_2 \end{bmatrix} \end{aligned} \quad (34)$$

which can be rearranged to obtain a linear polynomial equation $\mathbf{c}_0 + \mathbf{c}_1 t = 0$ which must be true for all $t \in [0, 1]$. This implies both vector-valued coefficients must be zero,

$$\begin{aligned} \mathbf{0} &= \mathbf{c}_0 = v_2 \mathbf{b}_{011} + v_1 \mathbf{b}_{020} + v_0 \mathbf{b}_{110} - \hat{\mathbf{b}}_{101} \\ \mathbf{0} &= \mathbf{c}_1 = -v_2 \mathbf{b}_{011} - v_1 \mathbf{b}_{020} + v_2 \hat{\mathbf{b}}_{101} - v_0 \mathbf{b}_{110} + v_1 \mathbf{b}_{110} + v_0 \mathbf{b}_{200} - \hat{\mathbf{b}}_{011} + \hat{\mathbf{b}}_{101} \end{aligned} \quad (35)$$

The solution is

$$\hat{\mathbf{b}}_{011} = v_0 \mathbf{b}_{200} + v_1 \mathbf{b}_{110} + v_2 \mathbf{b}_{101}, \quad \hat{\mathbf{b}}_{101} = v_0 \mathbf{b}_{110} + v_1 \mathbf{b}_{020} + v_2 \mathbf{b}_{011} \quad (36)$$

Figure 2 shows two pairs of subtriangles. Each pair is referred to as an *affine pair*. A given pair of subtriangles is coplanar, but the two planes for the two pairs are generally not the same plane. The use of the term *affine* refers to $\hat{\mathbf{b}}_{002}$, $\hat{\mathbf{b}}_{011}$ and $\hat{\mathbf{b}}_{101}$, all using the same barycentric coordinates (v_0, v_1, v_2) relative to the top domain triangle. I coined the phrase that the subtriangles are *coaffine*. Equations (27) and (36) guarantee that the first-order derivatives are continuous over the joint domain.

3 Globally C^1 Quadratic Height Field of Form $h = f(x_0, x_1)$ without Local Control

Equation (36) indicates that for a general triangle patch, there are 3 control points that can be arbitrarily chosen in the top triangle patch of figure 2. Once chosen, the 2 remaining control points in the bottom triangle patch are determined. However, more constraints are necessary when the patches are built for a height field. In the general case, $\hat{\mathbf{b}}_{011}$ and $\hat{\mathbf{b}}_{101}$ move about in space as the values of \mathbf{b}_{110} , \mathbf{b}_{101} and \mathbf{b}_{011} are modified. The projection of $\hat{\mathbf{b}}_{011}$ onto the domain triangle is not necessarily on the edge $\langle \mathbf{x}_{200}, \hat{\mathbf{x}}_{002} \rangle$. Similarly, the projection of $\hat{\mathbf{b}}_{101}$ onto the domain triangle is not necessarily on the edge $\langle \mathbf{x}_{020}, \hat{\mathbf{x}}_{002} \rangle$. To ensure that the projections are on the appropriate edges of the domain triangles, consider the following argument.

Let $\hat{\mathbf{x}}_{011}$ be the projection of $\hat{\mathbf{b}}_{011}$ onto the domain triangle and let $\hat{\mathbf{x}}_{101}$ be the projection of $\hat{\mathbf{b}}_{101}$ onto the domain triangle. To be on the edges, we need

$$\hat{\mathbf{x}}_{011} = (1 - \alpha) \mathbf{x}_{200} + \alpha \hat{\mathbf{x}}_{002}, \quad \hat{\mathbf{x}}_{101} = (1 - \beta) \mathbf{x}_{020} + \beta \hat{\mathbf{x}}_{002} \quad (37)$$

for some $\alpha \in (0, 1)$ and $\beta \in (0, 1)$. Let the projections of \mathbf{b}_I onto the domain plane be \mathbf{x}_I . We require that the projections lie on the appropriate edges of the domain triangle; that is,

$$\mathbf{x}_{110} = \gamma\mathbf{x}_{200} + (1 - \gamma)\mathbf{x}_{020}, \quad \mathbf{x}_{101} = \delta\mathbf{x}_{002} + (1 - \delta)\mathbf{x}_{200}, \quad \mathbf{x}_{011} = \epsilon\mathbf{x}_{020} + (1 - \epsilon)\mathbf{x}_{002} \quad (38)$$

for some $\gamma \in (0, 1)$, $\delta \in (0, 1)$ and $\epsilon \in (0, 1)$. We then have

$$\begin{aligned} \hat{\mathbf{x}}_{011} &= v_0\mathbf{x}_{200} + v_1\mathbf{x}_{110} + v_2\mathbf{x}_{101} \\ &= v_0\mathbf{x}_{200} + v_1[\gamma\mathbf{x}_{200} + (1 - \gamma)\mathbf{x}_{020}] + v_2[\delta\mathbf{x}_{002} + (1 - \delta)\mathbf{x}_{200}] \\ &= [v_0 + \gamma v_1 + (1 - \delta)v_2]\mathbf{x}_{200} + [(1 - \gamma)v_1]\mathbf{x}_{020} + [\delta v_2]\mathbf{x}_{002} \\ \hat{\mathbf{x}}_{011} &= (1 - \alpha)\mathbf{x}_{200} + \alpha\hat{\mathbf{x}}_{002} \\ &= (1 - \alpha)\mathbf{x}_{200} + \alpha(v_0\mathbf{x}_{200} + v_1\mathbf{x}_{020} + v_2\mathbf{x}_{002}) \\ &= [(1 - \alpha) + \alpha v_0]\mathbf{x}_{200} + [\alpha v_1]\mathbf{x}_{020} + [\alpha v_2]\mathbf{x}_{002} \end{aligned} \quad (39)$$

Equating the coefficients of the two equations involving $\hat{\mathbf{x}}_{011}$ leads to $\delta = \alpha = 1 - \gamma$. Substituting this into the edge equations (38), we obtain

$$\mathbf{x}_{110} = \delta\mathbf{x}_{020} + (1 - \delta)\mathbf{x}_{200}, \quad \mathbf{x}_{101} = \delta\mathbf{x}_{002} + (1 - \delta)\mathbf{x}_{200} \quad (40)$$

Subtracting the two equations,

$$\mathbf{x}_{110} - \mathbf{x}_{101} = \delta(\mathbf{x}_{020} - \mathbf{x}_{002}) \quad (41)$$

which says that the edges $\langle \mathbf{x}_{110}, \mathbf{x}_{101} \rangle$ and $\langle \mathbf{x}_{020}, \mathbf{x}_{002} \rangle$ are parallel. Therefore, the subtriangle $\langle \mathbf{x}_{200}, \mathbf{x}_{110}, \mathbf{x}_{101} \rangle$ and the original triangle $\langle \mathbf{x}_{200}, \mathbf{x}_{020}, \mathbf{x}_{002} \rangle$ are similar triangles.

The construction can be applied to the other cases to show that

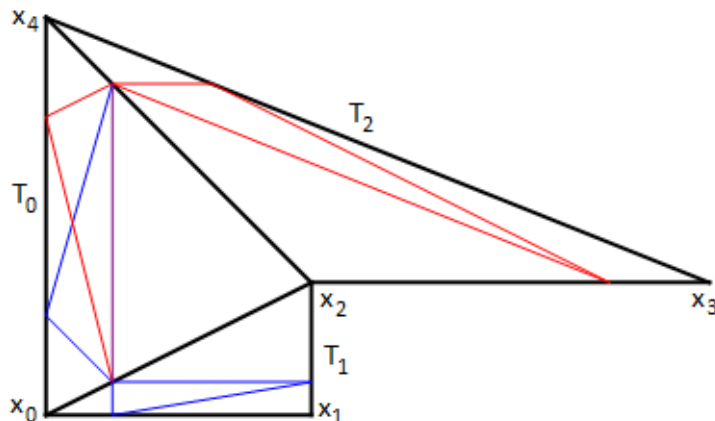
- The triangles $\langle \mathbf{x}_{200}, \mathbf{x}_{020}, \mathbf{x}_{002} \rangle$, $\langle \mathbf{x}_{200}, \mathbf{x}_{110}, \mathbf{x}_{101} \rangle$ and $\langle \mathbf{x}_{110}, \mathbf{x}_{020}, \mathbf{x}_{011} \rangle$ are similar.
- The triangles $\langle \hat{\mathbf{x}}_{200}, \hat{\mathbf{x}}_{020}, \hat{\mathbf{x}}_{002} \rangle$, $\langle \hat{\mathbf{x}}_{200}, \hat{\mathbf{x}}_{110}, \hat{\mathbf{x}}_{101} \rangle$ and $\langle \hat{\mathbf{x}}_{110}, \hat{\mathbf{x}}_{020}, \hat{\mathbf{x}}_{011} \rangle$ are similar.

For derivative continuity of a height field formed by triangle patches, we need the aforementioned similarity of triangles in addition to the constraints of equations (27) and (36).

In the general case for two adjacent triangle patches, we can freely choose the 3 control points \mathbf{b}_{110} , \mathbf{b}_{101} and \mathbf{b}_{011} , after which \hat{b}_{101} and \hat{b}_{011} are determined according to the construction presented here. In the height-field case, we can freely choose only 1 control point, say, \mathbf{b}_{110} , after which \mathbf{b}_{101} , \mathbf{b}_{011} , \hat{b}_{101} and \hat{b}_{011} are determined.

The degree of freedom in the height-field case is lost when a triangle in the mesh has at least 2 adjacent triangles. Figure 3 illustrates the problem.

Figure 3. Consider three domain triangles that define a piecewise quadratic height field. Domain triangle T_0 has two adjacent domain triangles, T_1 and T_2 . The colored subtriangles are attempts to subdivide the domain triangles to achieve a globally C^1 quadratic height field.

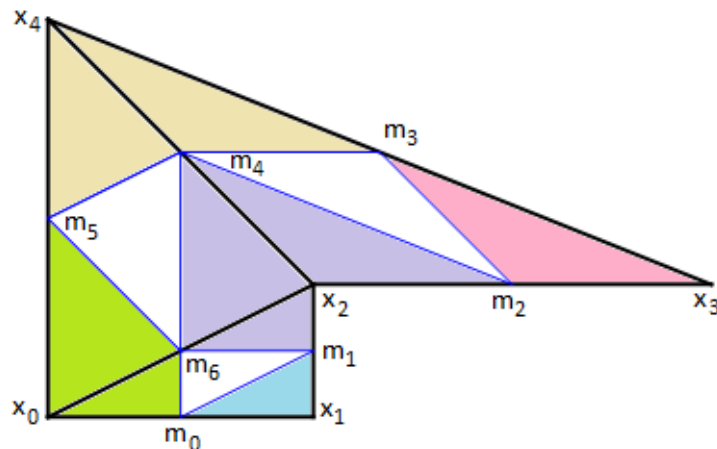


To ensure C^1 continuity along the shared edge $\langle \mathbf{x}_0, \mathbf{x}_2 \rangle$ of T_0 and T_1 , the previous construction allows us to choose any point on that edge as part of the subdivision. The figure shows a choice of $(3\mathbf{x}_0 + \mathbf{x}_2)/4$. The blue edges of T_1 are chosen to satisfy the similar-triangle condition required for C^1 continuity of the height field along the shared edge; those edges in T_1 emanating from the shared-edge point are parallel to the other edges of T_1 . Triangle T_0 has 2 blue edges and 1 purple edge emanating from the shared-edge point. These edges form the subdivision of T_0 that satisfies the similar-triangle condition of T_0 required for C^1 continuity of the height field along the shared edge. The blue and purple edges emanating from the shared-edge point are parallel to the appropriate edges of T_0 .

On the other hand, consider the shared edge of T_0 and T_2 . To obtain C^1 continuity along the shared edge of T_0 and T_1 , we are forced to use the point (as shown) of that edge. The red edges of T_2 are those that must be chosen for the subdivision of T_2 in order to satisfy the similar-triangle condition; the two red edges emanating from the shared-edge point are parallel to the appropriate edges of T_2 . Likewise, the edges of the subdivision of T_0 emanating from the shared-edge point must be parallel to the appropriate edges of T_0 . One of them is colored red, the other purple. The purple edge is the same as the one generated by C^1 continuity along the shared edge of T_0 and T_1 ; however, the red edge is not the same as the blue edge generated by C^1 continuity along the shared edge of T_0 and T_1 . Therefore, it is not possible to achieve global C^1 continuity using the originally chosen shared-edge point.

The adjacent triangles T_1 and T_2 require T_0 to have the 3 edges of the interior subtriangle parallel to the appropriate edges of T_0 . The only way this can happen is if we choose the midpoints of the edges for the subdivision. Figure 4 illustrates this.

Figure 4. Consider three domain triangles that define a piecewise quadratic height field. Domain triangle T_0 has two adjacent domain triangles, T_1 and T_2 . As long as we subdivide using edge midpoints, we can construct a globally C^1 quadratic height field.



No matter how many triangles are in the mesh, the similar-triangle conditions are satisfied for all triangles using subdivisions that involve only the edge midpoints. Each set of colored domain triangles represents the coplanarity of the 3D triangles. The light yellow triangles are an affine pair and the lime triangles are an affine pair. The vertex \mathbf{x}_2 is part of two affine pairs that are colored lavender, so all three subtriangles are coplanar. The light turquoise triangle and the rose triangle are not members of affine pairs.

Generally, a consequence of the edge-midpoint subdivision is that the domain portion of the interpolation is actually linear, not quadratic. To see this in the example, consider triangle T_0 that has vertices \mathbf{x}_0 , \mathbf{x}_1 and \mathbf{x}_2 . The domain portion of the interpolation is

$$\begin{aligned}
 \mathbf{x}(\mathbf{u}) &= \begin{bmatrix} u_0 & u_1 & u_2 \end{bmatrix} \begin{bmatrix} \mathbf{x}_2 & \mathbf{m}_6 & \mathbf{m}_1 \\ \mathbf{m}_6 & \mathbf{x}_0 & \mathbf{m}_0 \\ \mathbf{m}_1 & \mathbf{m}_0 & \mathbf{x}_1 \end{bmatrix} \begin{bmatrix} u_0 \\ u_1 \\ u_2 \end{bmatrix} \\
 \mathbf{x}(\mathbf{u}) &= \begin{bmatrix} u_0 & u_1 & u_2 \end{bmatrix} \begin{bmatrix} \mathbf{x}_2 & (\mathbf{x}_0 + \mathbf{x}_2)/2 & (\mathbf{x}_1 + \mathbf{x}_2)/2 \\ (\mathbf{x}_0 + \mathbf{x}_2)/2 & \mathbf{x}_0 & (\mathbf{x}_0 + \mathbf{x}_1)/2 \\ (\mathbf{x}_1 + \mathbf{x}_2)/2 & (\mathbf{x}_0 + \mathbf{x}_1)/2 & \mathbf{x}_1 \end{bmatrix} \begin{bmatrix} u_0 \\ u_1 \\ u_2 \end{bmatrix} \quad (42) \\
 &= u_0^2 \mathbf{x}_2 + u_1^2 \mathbf{x}_0 + u_2^2 \mathbf{x}_1 + u_0 u_1 (\mathbf{x}_0 + \mathbf{x}_2) + u_0 u_2 (\mathbf{x}_1 + \mathbf{x}_2) + u_1 u_2 (\mathbf{x}_0 + \mathbf{x}_1) \\
 &= u_0 (u_0 + u_1 + u_2) \mathbf{x}_2 + u_1 (u_0 + u_1 + u_2) \mathbf{x}_0 + u_2 (u_0 + u_1 + u_2) \mathbf{x}_1 \\
 &= u_0 \mathbf{x}_2 + u_1 \mathbf{x}_0 + u_2 \mathbf{x}_1
 \end{aligned}$$

where I have used the barycentric property that $u_0 + u_1 + u_2 = 1$. Without the reduction, you can view the

quadratic polynomial representing the domain variables as degree elevation of the linear polynomial. The height portion of the interpolation is quadratic and, generally, not reducible to a linear polynomial unless all the 3D control points are coplanar.

Let the known positions and heights in figure 4 be named (\mathbf{x}_i, f_i) for $0 \leq i \leq 4$. The midpoints are labeled \mathbf{m}_j for $0 \leq j \leq 6$. The heights at the midpoint are named h_i and are unknowns to be determined. Let the normal vectors to the purported tangent planes to the surface at the (\mathbf{x}_i, f_i) be named $(\mathbf{N}_i, -1)$, where $\mathbf{N}_i \in \mathbb{R}^2$. The normals are not necessarily unit length vectors, so the components of \mathbf{N}_i can be considered to be the first-order partial derivatives of the height field; that is, $\mathbf{N}_i = \nabla f_i$. The planes at the vertices are represented algebraically by $z = \mathbf{N}_i \cdot (\mathbf{x} - \mathbf{x}_i) + f_i$. The unknown heights are determined by

$$\begin{aligned}
h_0 &= \mathbf{N}_0 \cdot (\mathbf{m}_0 - \mathbf{x}_0) + f_0 = \mathbf{N}_1 \cdot (\mathbf{m}_0 - \mathbf{x}_1) + f_1 \\
h_1 &= \mathbf{N}_1 \cdot (\mathbf{m}_1 - \mathbf{x}_1) + f_1 = \mathbf{N}_2 \cdot (\mathbf{m}_1 - \mathbf{x}_2) + f_2 \\
h_2 &= \mathbf{N}_2 \cdot (\mathbf{m}_2 - \mathbf{x}_2) + f_2 = \mathbf{N}_3 \cdot (\mathbf{m}_2 - \mathbf{x}_3) + f_3 \\
h_3 &= \mathbf{N}_3 \cdot (\mathbf{m}_3 - \mathbf{x}_3) + f_3 = \mathbf{N}_4 \cdot (\mathbf{m}_3 - \mathbf{x}_4) + f_4 \\
h_4 &= \mathbf{N}_4 \cdot (\mathbf{m}_4 - \mathbf{x}_4) + f_4 = \mathbf{N}_2 \cdot (\mathbf{m}_4 - \mathbf{x}_2) + f_2 \\
h_5 &= \mathbf{N}_4 \cdot (\mathbf{m}_5 - \mathbf{x}_4) + f_4 = \mathbf{N}_0 \cdot (\mathbf{m}_5 - \mathbf{x}_0) + f_0 \\
h_6 &= \mathbf{N}_0 \cdot (\mathbf{m}_6 - \mathbf{x}_0) + f_0 = \mathbf{N}_2 \cdot (\mathbf{m}_6 - \mathbf{x}_2) + f_2
\end{aligned} \tag{43}$$

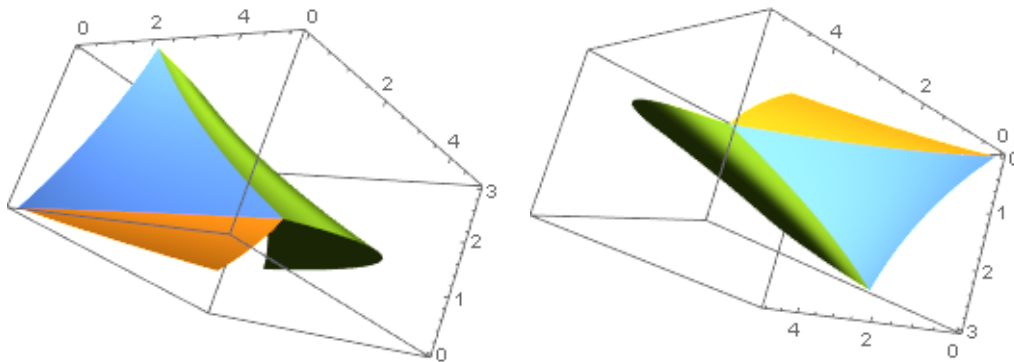
These provide 7 linear equations in the 10 unknown components of \mathbf{N}_i , so we expect to have 3 degrees of freedom for those components.

The degrees of freedom are better understood geometrically. Suppose we choose \mathbf{N}_0 arbitrarily, using up 2 of the 3 degrees of freedom. The tangent plane at \mathbf{x}_0 is now known, which in turn determines the heights h_0 , h_5 and h_6 because the points (\mathbf{m}_0, h_0) , (\mathbf{m}_5, h_5) and (\mathbf{m}_6, h_6) are on that plane. Now consider the tangent plane at \mathbf{x}_4 . We know that (\mathbf{x}_4, f_4) and (\mathbf{m}_5, h_5) are on that plane, which means that one of the components of \mathbf{N}_4 is determined. The other component is yet unknown, because the plane can rotate about the line containing the two known points on the plane. Choose that component (or choose a linear equation relating the two components), which uses the last of the degrees of freedom. The plane at \mathbf{x}_4 is known, which in turn determines the heights h_3 and h_4 because the points (\mathbf{m}_3, h_3) and (\mathbf{m}_4, h_4) are on that plane.

The points (\mathbf{x}_2, f_2) , (\mathbf{m}_4, h_4) and (\mathbf{m}_6, h_6) are all known, which determines the tangent plane at \mathbf{x}_2 . In turn, this plane determines h_1 and h_2 because the points (\mathbf{m}_1, h_1) and (\mathbf{m}_2, h_2) are on that plane. Finally, we now know the points (\mathbf{m}_0, h_0) , (\mathbf{x}_1, f_1) and (\mathbf{m}_1, h_1) , which determines the tangent plane at \mathbf{x}_1 . And we now know the points (\mathbf{m}_2, h_2) , (\mathbf{x}_3, f_3) and (\mathbf{m}_3, h_3) , which determines the tangent plane at \mathbf{x}_3 .

To illustrate using the triangles of figure 4, let $(\mathbf{x}_0, f_0) = ((0, 0), 0)$, $(\mathbf{x}_1, f_1) = ((2, 0), 3)$, $(\mathbf{x}_2, f_2) = ((2, 1), 4)$, $(\mathbf{x}_3, f_3) = ((5, 1), 1)$ and $(\mathbf{x}_4, f_4) = ((0, 3), 2)$. Choose $\mathbf{N}_0 = (1, 1)$ and $\mathbf{N}_1 = (\alpha, \beta)$ where $\alpha + \beta = 1$. Figure 5 shows the graph of the globally C^1 quadratic height field satisfying the aforementioned conditions.

Figure 5. Two views of the graph of a C^1 quadratic height field without local control. The domain of the height field is shown in figure 4.



4 Globally C^1 Quadratic Height Field of Form $h = f(x_0, x_1)$ with Local Control

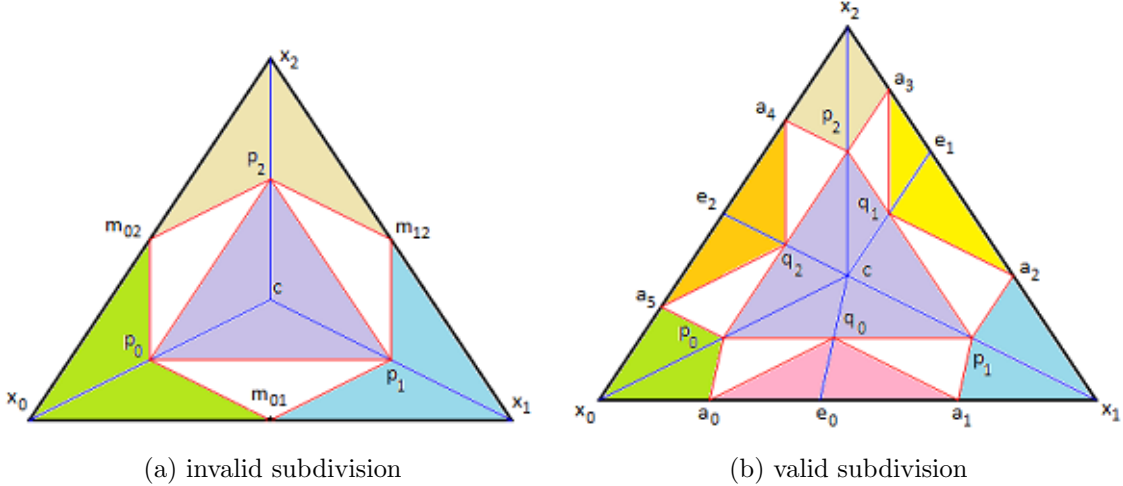
The example of the previous section is unappealing in that there are 3 degrees of freedom, forcing you to choose that freedom by selecting a normal vector at one vertex and imposing an arbitrary condition in order to determine the normals at the remaining vertices. More desirable is to have an algorithm that is symmetric in that each sample point has the same type of information. This can be accomplished by subdividing the triangles that occur in the domain triangulation of the samples in order to obtain more degrees of freedom. Some derivative information is required, even in the example of the previous section, so our goal is to have a set of samples of the form $(\mathbf{x}_i, f_i, \nabla f_i)$.

As a first attempt at subdivision, choose an interior point of a triangle and subdivide the triangle into 3 subtriangles by connecting the interior point to the 3 vertices. Each subtriangle is itself subdivided into 4 subtriangles using edge-midpoints for the subdivision. Figure 6 (a) shows the subdivision for a triangle $\langle \mathbf{x}_0, \mathbf{x}_1, \mathbf{x}_2 \rangle$ drawn using thick black lines. The interior point is \mathbf{c} . The first level of subdivision is drawn using blue lines. The \mathbf{m}_{ij} are the midpoints of the edges of the original triangle. The \mathbf{p}_i are the midpoints of the edges on which they live. The second level of subdivision is drawn using red lines. The samples are $(\mathbf{x}_i, f_i, \nabla f_i)$ for $0 \leq i \leq 2$. The tangent planes are therefore determined at the vertices of the original triangle. The colored regions indicate the subtriangles that are coplanar because of the coaffinity condition.

In figure 6 (a), the tangent plane at \mathbf{x}_0 determines the heights at \mathbf{m}_{01} and \mathbf{m}_{02} , the tangent plane at \mathbf{x}_1 determines the heights at \mathbf{m}_{01} and \mathbf{m}_{12} and the tangent plane at \mathbf{x}_2 determines the heights at \mathbf{m}_{12} and \mathbf{m}_{02} , all overconstrained problems.

In figure 6 (b), the problem is remedied by subdividing the original triangle into 6 subtriangles which are drawn using blue lines. Each of the 6 subtriangles is further subdivided using midpoints of edges, and these subtriangles are drawn using red lines. As we will see, the heights at the subdivision points are properly constrained.

Figure 6. (a) An attempt at subdivision to introduce more degrees of freedom in fitting the original triangle with a globally C^1 quadratic height field. The attempt fails because the heights h_{ij} at \mathbf{m}_{ij} are overconstrained. For example, the point $(\mathbf{m}_{01}, h_{01})$ must be a point on the two independent tangent planes at \mathbf{x}_0 and \mathbf{x}_1 . (b) An attempt at subdivision to introduce more degrees of freedom in fitting the original triangle with a globally C^1 quadratic height field. The attempt succeeds because the heights at the subdivision domain points are properly constrained.



The subdivision and height-fitting algorithm is described next, and is the material presented by Cendes and Wong [2]. Choose an interior point \mathbf{c} for the triangle. In barycentric coordinates,

$$\mathbf{c} = u_0\mathbf{x}_0 + u_1\mathbf{x}_1 + u_2\mathbf{x}_2 \quad (44)$$

for $u_i \in (0, 1)$ with $u_0 + u_1 + u_2 = 1$. Choose interior edge points \mathbf{e}_0 , \mathbf{e}_1 and \mathbf{e}_2 , which are not required to be midpoints of the original triangle's edges. In barycentric coordinates,

$$\mathbf{e}_0 = (1 - v_0)\mathbf{x}_0 + v_0\mathbf{x}_1, \quad \mathbf{e}_1 = (1 - v_1)\mathbf{x}_1 + v_1\mathbf{x}_2, \quad \mathbf{e}_2 = (1 - v_2)\mathbf{x}_2 + v_2\mathbf{x}_0 \quad (45)$$

for $v_i \in (0, 1)$. The remaining subdivision domain points are all midpoints of various line segments,

$$\begin{aligned} \mathbf{p}_0 &= (\mathbf{x}_0 + \mathbf{c})/2, & \mathbf{p}_1 &= (\mathbf{x}_1 + \mathbf{c})/2, & \mathbf{p}_2 &= (\mathbf{x}_2 + \mathbf{c})/2 \\ \mathbf{q}_0 &= (\mathbf{e}_0 + \mathbf{c})/2, & \mathbf{q}_1 &= (\mathbf{e}_1 + \mathbf{c})/2, & \mathbf{q}_2 &= (\mathbf{e}_2 + \mathbf{c})/2 \\ \mathbf{a}_0 &= (\mathbf{x}_0 + \mathbf{e}_0)/2, & \mathbf{a}_1 &= (\mathbf{e}_0 + \mathbf{x}_1)/2, & \mathbf{a}_2 &= (\mathbf{x}_1 + \mathbf{e}_1)/2 \\ \mathbf{a}_3 &= (\mathbf{e}_1 + \mathbf{x}_2)/2, & \mathbf{a}_4 &= (\mathbf{x}_2 + \mathbf{e}_2)/2, & \mathbf{a}_5 &= (\mathbf{e}_2 + \mathbf{x}_0)/2 \end{aligned} \quad (46)$$

The tangent plane at \mathbf{x}_0 is defined by $\nabla f_0 \cdot (\mathbf{x} - \mathbf{x}_0) + f_0$ and determines the heights at the subdivision points adjacent to \mathbf{x}_0 ; that is,

$$h_{\mathbf{p}_0} = \nabla f_0 \cdot (\mathbf{p}_0 - \mathbf{x}_0) + f_0, \quad h_{\mathbf{a}_0} = \nabla f_0 \cdot (\mathbf{a}_0 - \mathbf{x}_0) + f_0, \quad h_{\mathbf{a}_5} = \nabla f_0 \cdot (\mathbf{a}_5 - \mathbf{x}_0) + f_0 \quad (47)$$

The tangent plane at \mathbf{x}_1 is defined by $\nabla f_1 \cdot (\mathbf{x} - \mathbf{x}_1) + f_1$ and determines the heights at the subdivision points adjacent to \mathbf{x}_1 ; that is,

$$h_{\mathbf{p}_1} = \nabla f_1 \cdot (\mathbf{p}_1 - \mathbf{x}_1) + f_1, \quad h_{\mathbf{a}_1} = \nabla f_1 \cdot (\mathbf{a}_1 - \mathbf{x}_1) + f_1, \quad h_{\mathbf{a}_2} = \nabla f_1 \cdot (\mathbf{a}_2 - \mathbf{x}_1) + f_1 \quad (48)$$

The tangent plane at \mathbf{x}_2 is defined by $\nabla f_2 \cdot (\mathbf{x} - \mathbf{x}_2) + f_2$ and determines the heights at the subdivision points adjacent to \mathbf{x}_2 ; that is,

$$h_{\mathbf{p}_2} = \nabla f_2 \cdot (\mathbf{p}_2 - \mathbf{x}_2) + f_2, \quad h_{\mathbf{a}_3} = \nabla f_2 \cdot (\mathbf{a}_3 - \mathbf{x}_2) + f_2, \quad h_{\mathbf{a}_4} = \nabla f_2 \cdot (\mathbf{a}_4 - \mathbf{x}_2) + f_2 \quad (49)$$

The points $(\mathbf{p}_i, h_{\mathbf{p}_i})$ are now known for $0 \leq i \leq 2$ and they are necessarily coplanar. This plane determines the heights at \mathbf{q}_i and \mathbf{c} ,

$$\begin{aligned} h_{\mathbf{q}_0} &= (1 - v_0)h_{\mathbf{p}_0} + v_0h_{\mathbf{p}_1}, \quad h_{\mathbf{q}_1} = (1 - v_1)h_{\mathbf{p}_1} + v_1h_{\mathbf{p}_2}, \quad h_{\mathbf{q}_2} = (1 - v_2)h_{\mathbf{p}_2} + v_2h_{\mathbf{p}_0} \\ h_{\mathbf{c}} &= u_0h_{\mathbf{p}_0} + u_1h_{\mathbf{p}_1} + u_2h_{\mathbf{p}_2} \end{aligned} \quad (50)$$

The height equations use the following facts that are simple to prove algebraically (or by similarity of triangles and parallelograms),

$$\begin{aligned} \mathbf{q}_0 &= (1 - v_0)\mathbf{p}_0 + v_0\mathbf{p}_1, \quad \mathbf{q}_1 = (1 - v_1)\mathbf{p}_1 + v_1\mathbf{p}_2, \quad \mathbf{q}_2 = (1 - v_2)\mathbf{p}_2 + v_2\mathbf{p}_0 \\ \mathbf{c} &= u_0\mathbf{p}_0 + u_1\mathbf{p}_1 + u_2\mathbf{p}_2 \end{aligned} \quad (51)$$

The points $(\mathbf{q}_i, h_{\mathbf{q}_i})$ are now known for $0 \leq i \leq 2$ and the points $(\mathbf{a}_i, h_{\mathbf{a}_i})$ are now known for $0 \leq i \leq 5$. This information determines the points $(\mathbf{e}_i, h_{\mathbf{e}_i})$ for $0 \leq i \leq 2$, each point living on a plane formed by a \mathbf{q} -vector and two \mathbf{a} -vectors. Specifically,

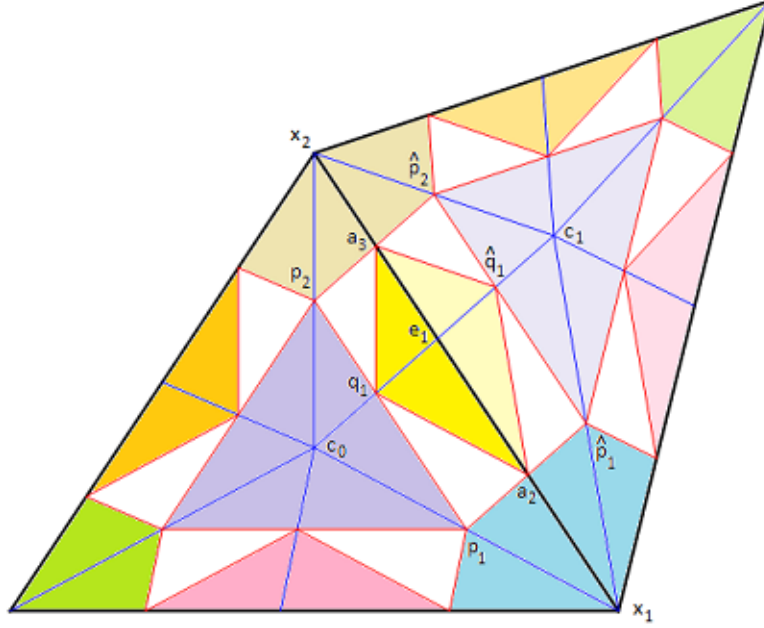
$$h_{\mathbf{e}_0} = (1 - v_0)h_{\mathbf{a}_0} + v_0h_{\mathbf{a}_1}, \quad h_{\mathbf{e}_1} = (1 - v_1)h_{\mathbf{a}_2} + v_1h_{\mathbf{a}_3}, \quad h_{\mathbf{e}_2} = (1 - v_2)h_{\mathbf{a}_4} + v_2h_{\mathbf{a}_5} \quad (52)$$

The height equations use the following facts that are simple to prove algebraically (or by similarity of triangles),

$$\mathbf{e}_0 = (1 - v_0)\mathbf{a}_0 + v_0\mathbf{a}_1, \quad \mathbf{e}_1 = (1 - v_1)\mathbf{a}_2 + v_1\mathbf{a}_3, \quad \mathbf{e}_2 = (1 - v_2)\mathbf{a}_4 + v_2\mathbf{a}_5 \quad (53)$$

The previous equations determine the subdivision points and heights that lead to a C^1 quadratic height field. However, we must now prove that two adjacent triangles, both subdivided accordingly, form a C^1 quadratic height field. Figure 7 shows two such triangles. The figure has labels only for the subdivision domain points that affect influence the derivative continuity. We know the domain point equations for the left triangle. For the right triangle we have $\hat{\mathbf{p}}_1 = (\mathbf{x}_1 + \mathbf{c}_1)/2$, $\hat{\mathbf{p}}_2 = (\mathbf{x}_2 + \mathbf{c}_2)/2$ and $\hat{\mathbf{q}}_1 = (1 - v_1)\hat{\mathbf{p}}_1 + v_1\hat{\mathbf{p}}_2$. The heights at those points are $h_{\hat{\mathbf{p}}_1} = \nabla f_1 \cdot (\hat{\mathbf{p}}_1 - \mathbf{x}_1) + f_1$, $h_{\hat{\mathbf{p}}_2} = \nabla f_2 \cdot (\hat{\mathbf{p}}_2 - \mathbf{x}_2) + f_2$ and $h_{\hat{\mathbf{q}}_1} = (1 - v_1)h_{\hat{\mathbf{p}}_1} + v_1h_{\hat{\mathbf{p}}_2}$.

Figure 7. Two adjacent triangles whose subdivisions form C^1 quadratic height fields. We need to prove that their first-order derivatives match along the shared edge.



Each colored polygonal region represents control points that are coplanar. The lime, orange, rose, turquoise and violet regions of the left triangle are each associated with coplanar control points based on the analysis of the triangle in figure 6. The same is true for the lighter-colored regions of the right triangle.

The turquoise region containing (\mathbf{x}_1, f_1) spans both original triangles, two subtriangles from each of the original triangles. The control points adjacent to that of \mathbf{x}_1 are coplanar simply because we specified ∇f_1 at \mathbf{x}_1 . The tan region containing (\mathbf{x}_2, f_2) also spans both original triangles because we specified ∇f_2 at \mathbf{x}_2 .

The derivative continuity along the shared edge hinges on whether the control points of the yellow region of the left triangle and the control points of the lighter-yellow region of the right triangle are coplanar. The coaffinity requirement for continuous derivatives is already supported by the subdivision having the correctly paired similar triangles. Cendes and Wong argued that the combined yellow regions is coplanar using a geometric argument. The proof here uses an algebraic because it naturally extends to higher dimensional extensions of the algorithm.

The domain point \mathbf{e}_1 is the intersection of the shared edge $\langle \mathbf{x}_1, \mathbf{x}_2 \rangle$ and the segment connecting the interior domain points $(\mathbf{c}_0, \mathbf{c}_1)$. To ensure that the intersection exists no matter what pair of triangles is considered, we can choose the \mathbf{c} -points to be the centers of inscribed circles for the triangles. The proof of existence of the intersection was given in Section 2.2. We may therefore write the intersection point as barycentric combinations,

$$\mathbf{e}_1 = (1 - t)\mathbf{c}_0 + t\mathbf{c}_1 = (1 - t)\mathbf{q}_1 + t\hat{\mathbf{q}}_1 \quad (54)$$

for some $t \in (0, 1)$. The last equality uses $\mathbf{q}_1 = (\mathbf{c}_0 + \mathbf{e}_1)/2$ and $\hat{\mathbf{q}}_1 = (\mathbf{c}_1 + \mathbf{e}_1)/2$. The height at \mathbf{e}_1 is

$$\begin{aligned} h_{\mathbf{e}_1} &= (1 - v_1)h_{\mathbf{a}_2} + v_1h_{\mathbf{a}_3} \\ &= (1 - v_1)[\nabla f_1 \cdot (\mathbf{a}_2 - \mathbf{x}_1) + f_1] + v_1[\nabla f_2 \cdot (\mathbf{a}_3 - \mathbf{x}_2) + f_2] \\ &= (1 - v_1)[\nabla f_1 \cdot (\mathbf{e}_1 - \mathbf{x}_1)/2 + f_1] + v_1[\nabla f_2 \cdot (\mathbf{e}_1 - \mathbf{x}_2)/2 + f_2] \end{aligned} \quad (55)$$

the height at \mathbf{q}_1 is

$$\begin{aligned} h_{\mathbf{q}_1} &= (1 - v_1)h_{\mathbf{p}_1} + v_1h_{\mathbf{p}_2} \\ &= (1 - v_1)[\nabla f_1 \cdot (\mathbf{p}_1 - \mathbf{x}_1) + f_1] + v_1[\nabla f_2 \cdot (\mathbf{p}_2 - \mathbf{x}_2) + f_2] \\ &= (1 - v_1)[\nabla f_1 \cdot (\mathbf{c}_0 - \mathbf{x}_1)/2 + f_1] + v_1[\nabla f_2 \cdot (\mathbf{c}_0 - \mathbf{x}_2)/2 + f_2] \end{aligned} \quad (56)$$

and the height at $\hat{\mathbf{q}}_1$ is

$$\begin{aligned} h_{\hat{\mathbf{q}}_1} &= (1 - v_1)h_{\hat{\mathbf{p}}_1} + v_1h_{\hat{\mathbf{p}}_2} \\ &= (1 - v_1)[\nabla f_1 \cdot (\hat{\mathbf{p}}_1 - \mathbf{x}_1) + f_1] + v_1[\nabla f_2 \cdot (\hat{\mathbf{p}}_2 - \mathbf{x}_2) + f_2] \\ &= (1 - v_1)[\nabla f_1 \cdot (\mathbf{c}_1 - \mathbf{x}_1)/2 + f_1] + v_1[\nabla f_2 \cdot (\mathbf{c}_1 - \mathbf{x}_2)/2 + f_2] \end{aligned} \quad (57)$$

Combining the last two heights,

$$\begin{aligned} (1 - t)h_{\mathbf{q}_1} + th_{\hat{\mathbf{q}}_1} &= (1 - t)(1 - v_1)[\nabla f_1 \cdot (\mathbf{c}_0 - \mathbf{x}_1)/2 + f_1] + v_1[\nabla f_2 \cdot (\mathbf{c}_0 - \mathbf{x}_2)/2 + f_2] \\ &\quad + t(1 - v_1)[\nabla f_1 \cdot (\mathbf{c}_1 - \mathbf{x}_1)/2 + f_1] + v_1[\nabla f_2 \cdot (\mathbf{c}_1 - \mathbf{x}_2)/2 + f_2] \\ &= (1 - v_1)[\nabla f_1 \cdot ((1 - t)\mathbf{c}_0 + t\mathbf{c}_1 - (1 - t)\mathbf{x}_1 - t\mathbf{x}_1)/2 + (1 - t)f_1 + tf_1] \\ &\quad + v_1[\nabla f_2 \cdot ((1 - t)\mathbf{c}_0 + t\mathbf{c}_1 - (1 - t)\mathbf{x}_2 - t\mathbf{x}_2)/2 + (1 - t)f_2 + tf_2] \\ &= (1 - v_1)[\nabla f_1 \cdot (\mathbf{e}_1 - \mathbf{x}_1)/2 + f_1] + v_1[\nabla f_2 \cdot (\mathbf{e}_1 - \mathbf{x}_2)/2] \\ &= h_{\mathbf{e}_1} \end{aligned} \quad (58)$$

In terms of the control points,

$$(\mathbf{e}_1, h_{\mathbf{e}_1}) = ((1 - t)\mathbf{q}_1 + t\hat{\mathbf{q}}_1, (1 - t)h_{\mathbf{q}_1} + th_{\hat{\mathbf{q}}_1}) = (1 - t)(\mathbf{q}_1, h_{\mathbf{q}_1}) + t(\hat{\mathbf{q}}_1, h_{\hat{\mathbf{q}}_1}) \quad (59)$$

which proves that the control points $(\mathbf{e}_1, h_{\mathbf{e}_1})$, $(\mathbf{q}_1, h_{\mathbf{q}_1})$ and $(\hat{\mathbf{q}}_1, h_{\hat{\mathbf{q}}_1})$ are collinear. This fact together with the coplanarity of $\{\mathbf{q}_1, \mathbf{a}_2, \mathbf{a}_3, \mathbf{e}_1\}$ and the coplanarity of $\{\hat{\mathbf{q}}_1, \mathbf{a}_2, \mathbf{a}_3, \mathbf{e}_1\}$ imply that $\{\mathbf{q}_1, \mathbf{a}_2, \mathbf{a}_3, \mathbf{e}_1, \hat{\mathbf{q}}_1\}$ are coplanar. In summary, the 4 subtriangles in the yellow-colored regions of figure 7 are coplanar which implies that the two quadratic Bézier triangle patches have continuous derivatives on the shared boundary.

5 The Algorithm for Graphs of $f(x, y, z)$

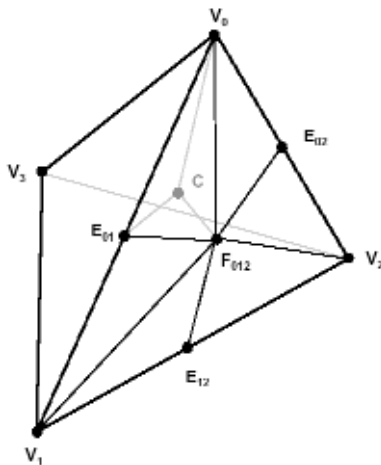
The Cendes-Wong algorithm may be extended to the interpolation of graphs of functions of three variables.

It is assumed that the 3D points have been tetrahedralized. Consider a tetrahedron whose vertices are V_i , $0 \leq i \leq 3$. Let C be the center of the inscribed sphere for the tetrahedron. Let F_{ijk} be a point on the face

with vertices V_i , V_j , and V_k . If the face is shared with another tetrahedron, let F_{ijk} be the intersection of that face and the line connecting the inscribed centers of the tetrahedra sharing that face. If the face is not shared, let F_{ijk} be the average of the vertices for that face. Let E_{ij} be the midpoint of the edge joining vertices V_i and V_j where $i < j$. Such a consistent choice, when multiple tetrahedra share the same edge, allows the construction of the Bézier net without having to analyze neighbor relationships. However, if only two tetrahedra share the same edge, then any interior edge point suffices.

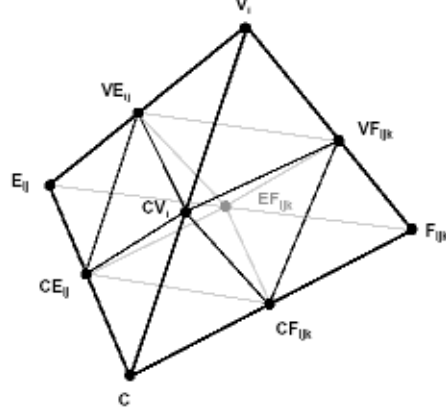
The tetrahedron can be subdivided into 24 smaller tetrahedrons, each having four vertices consisting of C , a vertex V_i , an edge point E_{ij} , and a face point F_{ijk} . Figure 8 shows a typical tetrahedron and one subtetrahedron.

Figure 8. Subdivision of a tetrahedron.



Each face of a subtetrahedron is partitioned into four Bézier triangles by selecting the midpoints of each of the edges. Figure 9 shows the labeling of those midpoints.

Figure 9. Subdivision of a subtetrahedron.



The equations relating all the labeled points are given below.

$$\begin{aligned}
 C &= c_0V_0 + c_1V_1 + c_2V_2 + c_3V_3; \quad c_i \geq 0, \quad c_0 + c_1 + c_2 + c_3 = 1 && 1 \text{ equation} \\
 F_{ijk} &= f_0V_i + f_1V_j + f_2V_k; \quad f_i \geq 0, \quad f_0 + f_1 + f_2 = 1 && 4 \text{ equations} \\
 E_{ij} &= (V_i + V_j)/2 && 6 \text{ equations} \\
 VE_{ij} &= (V_i + E_{ij})/2 && 12 \text{ equations} \\
 VF_{ijk} &= (V_i + F_{ijk})/2 && 12 \text{ equations} \\
 CV_i &= (C + V_i)/2 && 4 \text{ equations} \\
 CE_{ij} &= (E_{ij} + C)/2 && 6 \text{ equations} \\
 CF_{ijk} &= (C + F_{ijk})/2 && 4 \text{ equations} \\
 EF_{ijk} &= (E_{ij} + F_{ijk})/2 && 12 \text{ equations}
 \end{aligned} \tag{60}$$

There are a total of 61 equations relating the points. The same number of equations relates the sample values at those points. Compare this to the 19 values in the 2-dimensional case.

It is also assumed that at each vertex a function value and gradient have been specified. At vertex V_i let the function value be ϕ_{V_i} and let the gradient vector be $\nabla\phi_{V_i}$. The remaining sample values will be denoted ϕ_P where P is one of the points mentioned previously. To guarantee derivative continuity at a vertex, the Bézier net about that vertex must be covolumetric. This is possible by choosing

$$\begin{aligned}
 \phi_{VE_{ij}} &= \phi_{V_i} + \nabla\phi_{V_i} \cdot (VE_{ij} - V_i) \\
 \phi_{VF_{ijk}} &= \phi_{V_i} + \nabla\phi_{V_i} \cdot (VF_{ijk} - V_i) \\
 \phi_{CV_i} &= \phi_{V_i} + \nabla\phi_{V_i} \cdot (C - V_i)
 \end{aligned} \tag{61}$$

From these equations and the barycentric relationships, it follows that

$$\begin{aligned}
\phi_{F_{ijk}} &= f_0\phi_{VF_{ijk}} + f_1\phi_{VF_{jki}} + f_2\phi_{VF_{kij}} \\
\phi_C &= c_0\phi_{CV_0} + c_1\phi_{CV_1} + c_2\phi_{CV_2} + c_3\phi_{CV_3} \\
\phi_{CF_{ijk}} &= f_0\phi_{CV_i} + f_1\phi_{CV_j} + f_2\phi_{CV_k}
\end{aligned} \tag{62}$$

To guarantee derivative continuity along the edges, we need

$$\phi_{E_{ij}} = (\phi_{VE_{ij}} + \phi_{VE_{ji}})/2 \tag{63}$$

The $1/2$ factor occurs because E_{ij} was chosen as the midpoint between two vertices, so it is also the midpoint between VE_{ij} and VE_{ji} . Also note that $\phi_{E_{ij}}$ must depend only on function values at V_i and V_j since it is possible for arbitrarily many tetrahedrons to share an edge. Any dependence of an edge value on a particular tetrahedron would invalidate the construction.

It is also necessary that the subtetrahedrons containing the edge between VE_{ij} and VE_{ji} are covolumetric. Define

$$\nabla\phi_{ij} = \frac{\phi_{VE_{ij}} - \phi_{VE_{ji}}}{|VE_{ij} - VE_{ji}|^2} (VE_{ij} - VE_{ji}) \tag{64}$$

The remaining sample values are determined by

$$\begin{aligned}
\phi_{CE_{ij}} &= \phi_{E_{ij}} + \nabla\phi_{ij} \cdot (C - E_{ij}) \\
\phi_{EF_{ijk}} &= \phi_{E_{ij}} + \nabla\phi_{ij} \cdot (EF_{ijk} - E_{ij})
\end{aligned} \tag{65}$$

The argument of coaffinity is the same as in the 2D case: covolumetricity and midpoint subdivision imply coaffinity. However, this is more challenging to visualize since the covolumetricity refers to two 3-dimensional tetrahedrons belonging to the same 3-dimensional hyperplane which lives in 4D.

6 The Algorithm for Surfaces

This section is a description of an extension of the Cendes-Wong algorithm to triangular meshes which are not necessarily the graph of a function. If mesh is assumed to be sample from a parameterized surface $(x(s, t), y(s, t), z(s, t))$, the mesh vertices are of the form $\mathbf{V}_i = (x_i, y_i, z_i; s_i, t_i)$ where the vertex position is (x_i, y_i, z_i) and the surface parameters (texture coordinates, so to speak) are (s_i, t_i) . Each component $x(s, t)$, $y(s, t)$ and $z(s, t)$ is a height field of the surface parameters. The Cendes-Wong algorithm can be applied to each component separately to generate a globally C^1 interpolated surface.

If surface parameters are not known at the mesh vertices, they can be generated using concepts found in [1]. Of course, the topology of the mesh is important in selecting the parameterization algorithm.

References

- [1] Mario Botsch, Leif Kobbelt, Mark Pauly, Pierre Alliez, and Bruno Lévy. *Polygon Mesh Processing*. AK Peters Ltd., Natick, MA, 2010.

- [2] Zoltan J. Cendes and Steven H. Wong. C1 quadratic interpolation over arbitrary point sets. *IEEE Computer Graphics and Applications*, 7(11):8–16, November 1987.
- [3] Gerald Farin. *Curves and Surfaces for Computer Aided Geometric Design: A Practical Guide*. Academic Press, Inc., San Diego, CA, 1990.
- [4] Dave F. Watson. Computing the n-dimensional Delaunay tessellation with application to Voronoi polytopes. *The Computer Journal*, 24(2):167–172, 1981.